Friction on the Nanoscale and the Breakdown of Continuum Mechanics

Andrew Musser
Zernike Institute for Advanced Materials, University of Groningen, Nijenborgh 4, 9747 AG Groningen, The Netherlands
Dated: 01 May 2009

The fundamental laws of friction have been under study since the time of Leonardo da Vinci, but the micro- and nanoscopic mechanisms remain unclear. In the 20th century significant progress was made using continuum mechanics theories of contact. However, the validity of these theories at small length scales is uncertain. More recent atomic force microscopy and molecular dynamics simulation studies of friction on the nanoscale have disagreed with the continuum models and called some of the basic tenets of friction theory into question. After a brief presentation of the relevant continuum mechanics models of contact and friction, this paper will discuss the results of key atomic force microscope and molecular dynamics studies. It will be seen that while continuum models of friction are often misapplied and need further development, announcements of the breakdown of continuum mechanics are premature.

1 - Introduction

Elucidation of the laws governing friction represents one of the longest-standing problems in physics – the first systematic studies were performed by Leonardo da Vinci, and in 1699 Amontons published the first known laws of friction, which were subsequently developed further by Coulomb. The three Amontons-Coulomb laws[*], that the frictional force between two bodies is directly proportional to load and independent of contact area and sliding velocity, have formed the basis of all subsequent theories. And yet, after 300 years of study, particularly intensive in the latter half of the 20th century, a precise theory of friction accurate on all length scales remains elusive. Indeed, the development of increasingly advanced and powerful microscopies has primarily served to highlight the insufficiency of current ideas about friction, most of which are based on decades-old continuum mechanics theories describing contact

[*] Coulomb's primary contribution regarded the velocity dependence of friction, which is beyond the scope of this paper; the laws regarding area and load dependence will be denoted as "Amontons' laws".

between two ideal surfaces. This is especially true today with the recent advent and growth of nanoscience. A clear understanding of whether and how continuum models of friction break down at nanometer and atomic length scales will be critical to the development of devices on the micro- and nanoscales and the extraction of useful material information from atomic-scale friction microscopies,[1] and the current debate about this breakdown shall be the subject of this paper.

2 - Continuum Theories of Friction

Though tribology had long been an active field of inquiry, it was the publication of Bowden and Tabor's seminal work in 1954 that laid the foundations for the rigorous mathematical study of friction.[2] Bowden and Tabor realized that Amontons' laws had been developed with reference to only a projected contact area, whereas real macroscopic contact is between rough surfaces. They proposed to treat friction as arising from the plastic deformation of interlocking spherical asperities with the result that the frictional force is proportional to the total 'real' contact area defined by the deformation of the individual asperities. They also addressed friction in terms of purely elastic processes, focusing on the deformation of a single asperity according to Hertz contact theory, and concluded that under applied load L the lateral friction force $F_{lat} \sim L^{2/3}$, which contradicts Amontons' first law. While these results were important in their own right for linking the concepts of adhesion and friction, their more significant consequence was to spark further investigations of friction in terms of both single- and multi-asperity contact.

2.1 - Single-Asperity Contact Mechanics

The concept of real contact area and its relation to friction led to a focus on the behavior of individual asperities under contact and a re-examination of Hertz contact theory. Hertz[3] derived the elastic contact area of two hard spheres with radii of curvature R_1 and R_2, Young's moduli E_1 and E_2 and Poisson's ratios ν_1 and ν_2, pressed together with load L in the absence of adhesive forces as

$$A_{Hertz} = \pi \left(\frac{RL}{K} \right)^{2/3} \tag{1}$$

where $R = R_1 R_2 / (R_1 + R_2)$ and $K = \frac{4}{3}\left[\left(1 - \nu_1^2\right)/E_1 + \left(1 - \nu_2^2\right)/E_2 \right]$.* This has received ample verification on the macro scale, but it was realized that on sufficiently small length scales the relative importance of surface versus bulk effects would shift and the surface energy would play a significant role in contact.

Johnson, Kendall and Roberts (JKR) took this explicitly into account in a modification of the Hertz theory in which adhesion was assumed to only have an effect in the zone of intimate contact and was treated in terms of an interfacial surface free energy.[4] By minimizing the total energy of the system – elastic and surface energy and applied work – they found a larger contact area,

$$A_{JKR} = \pi \left[\frac{R}{K} \left(L + 3\gamma\pi R + \sqrt{6\gamma\pi RL + \left(3\gamma\pi R\right)^2} \right) \right]^{2/3} \tag{2}$$

where γ is the total surface free energy at contact given by $\gamma = \gamma_1 + \gamma_2 - \gamma_{12}$, γ_1 and γ_2 denoting the free energy of each surface and γ_{12} that of the interface. Two key consequences of adhesion evident in this expression are a finite contact area under zero applied load and a finite pull-off force, also with a finite contact area, given by $L_{c\,JKR} = -\frac{3}{2}\gamma\pi R$, though the Hertz expressions are recovered for $\gamma = 0$. Another noteworthy result of this formulation is the pressure distribution in the zone of contact: as seen in Figure 1, the tip is under compressive stress at the center and experiences a continuous transition to infinite tensile

* Unless otherwise noted, this notation will be used throughout this report.

stress at the contact edge. This discontinuity leads to a sharp bend in the material which was not observed in practice. Nonetheless the theory was found to adequately describe the contact behavior of relatively soft materials.

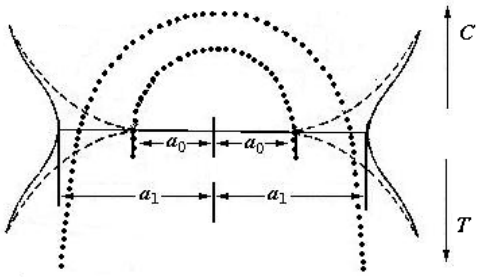

Figure 1. Contrasting the Hertz and JKR models. The dashed curves show the deformation profiles for two elastic spheres contacting without adhesion, with contact radius a_0; solid curves show the same system with adhesion, yielding a larger contact radius a_1. Dotted lines are the pressure distribution for each regime, where *C* indicates compressive and *T* tensile stress. Adapted from (4)

This theory was soon followed by a completely different approach to the problem of adhesive contact by Derjaguin, Muller and Toporov (DMT).[5] Two spheres were assumed to deform according to Hertz contact mechanics, and no additional adhesive force was considered within the zone of intimate contact on the grounds that such forces were already accounted for by Hertz. Instead, a more physical, longer-range attractive force than that of the JKR theory was proposed to act in an annulus between the contact radius a_{DMT} and some radius c determined by the separation of the two spheres. Denoting this load- and geometry-dependent adhesive force as F_{ad}, the area of contact is then given by

$$A_{DMT} = \pi\left(\frac{R\left(L+F_{ad}\right)}{K}\right)^{2/3} \tag{3}$$

which is once again finite at zero applied load, though with a smaller contact radius than in the JKR case given the same adhesive force. This contact area decreases continuously to zero, yielding a finite pull-off force of $L_{cDMT} = -2\gamma\pi R$, a factor of $4/3$ greater than in the JKR theory.

A direct comparison and evaluation of these models proved elusive due to the difficulty of precisely measuring areas of contact and the surface free energy, and for several years they were in direct competition until Tabor proposed that the JKR and DMT regimes are opposite extremes of essentially the same behavior.[6] He developed another model of adhesive contact assuming extremely short-range attractive forces, with results similar to the JKR model. The nature of the forces considered resulted in the contact zone being formed at the end of a vertically extended 'neck' along the lines of that depicted in Figure 2, which led Tabor to the conclusion that the assumptions he had made would only be valid in the limit that the sphere-plane separation outside of the neck was greater than the range of the attractive forces being considered (several atomic diameters). This condition is easily satisfied by soft rubber-like

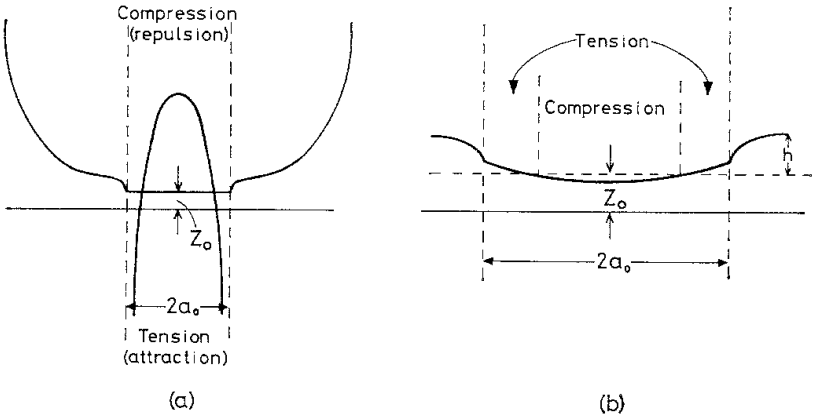

Figure 2. Single-asperity deformation of a soft sphere with contact radius a_0 and equilibrium separation Z_0 (a) with an overlay of the pressure distribution, and (b) greatly exaggerated to demonstrate the zones of compressive and tensile stress and the contact neck with height *h*. From (6)

materials but fails for hard, rigid systems. Considering these systems in terms of microasperities of varying heights (i.e. roughness) pressing elastically into a substrate, Tabor deduced that the correct regime of adhesive contact could be determined from a ratio of material properties expressing a balance between adhesive forces on short microasperities and the elastic energy cost of tall asperities penetrating into another material. This ratio is commonly known as Tabor's parameter, and it is extensively used to approximate the applicability of the JKR and DMT models – a large value, typically greater than 5, corresponds to soft materials with strong short-range attractive forces (JKR), while stiff materials with relatively weak, longer-range attractive forces (DMT) give values below 0.1.

The intermediate range of Tabor's parameter proved much more resistant to theoretical description, restricted for many years to various self-consistent calculations of limited experimental utility.[7,8] However, in 1991 Maugis applied concepts of fracture mechanics to the problem of adhesion and contact and, using a Dugdale potential, produced an analytical description of the intermediate regime that avoids self-consistent calculations and produces the DMT and JKR results in the appropriate limits.[9] Rather than a realistic force law such as the Lennard-Jones (L-J) potential, this model assumes constant adhesion forces between the surfaces in an annulus between radii a (the intimate contact zone) and c (the outer extent of the attractive interactions) for computational simplicity. This constraint and the balance between the surface free energy of the contact γ and the strain energy released around the contact zone when the crack area varies by dA are sufficient to determine the relation between experimental parameters. The mathematics is cumbersome, and use of the equations requires extensive numerical calculations, but it can be shown that varying a parameter based on the ratio c/a gives a smooth transition from JKR ($c/a \approx 1$) to DMT behavior ($c/a >> 1$) for single-asperity stress distributions and deformation profiles. This parameter is closely related to Tabor's parameter.

Carpick, Ogletree and Salmeron (COS) developed an empirical fit to this model[10] which was later given a physical explanation by Schwarz[11] and allowed easier application of the Maugis-Dugdale (M-D) model to experimental data. Because of the similarity of the JKR and DMT expressions for contact area as a function of load, they are combined in a single equation with a dimensionless empirical transition parameter α ranging from 0 (DMT) to 1 (JKR):

$$\frac{A}{A_{0(\alpha)}} = \left(\frac{\alpha + \sqrt{1 - L/L_{c(\alpha)}}}{1+\alpha} \right)^{2/3} \qquad (4)$$

where $A_{0(\alpha)}$ is the zero-load contact area for the corresponding regime. The resulting equations for stress distribution and tip deformation closely match the M-D solutions throughout the intermediate range, generally to within 1%. The physical justification of this model entails separating the full work of adhesion into two parts, as shown in Figure 3: one reflects work against short-range forces and is modeled as a delta function, while the other captures the effect of diffuse longer-range interactions. Changing the balance of these two contributions effects a smooth transition from the JKR the DMT regimes for contact radius as a function of load, tip deformation and radial pressure distribution.

This simplified form of the M-D model and the DMT and JKR theories still see significant application today as reasonable approximations of the interaction of an AFM tip with a surface. However, it must be stressed that these models are strictly only applicable for linear elastic materials with perfectly smooth surfaces. As continuum theories they are not designed to take the atomic nature of matter into account,

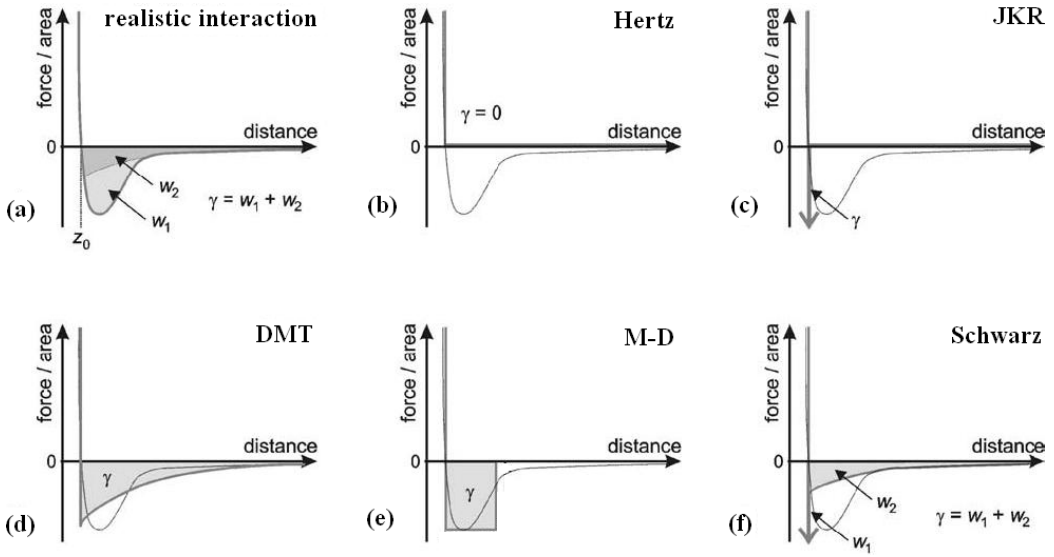

Figure 3. The interaction forces used in single-asperity contact models, as functions of surface separation. (a) depicts a realistic interaction, with the work of adhesion, denoted γ, separated into two parts attributed to short-range (w_1) and long-range (w_2) forces. For comparison, the force curve from (a) is reproduced in grey in (b-f). All model interactions (b-f) include a δ -function hard-wall repulsion at z_0. Additionally, the JKR and Schwarz models include δ -function attractive interactions at z_0. From (11)

and indeed none of them even explicitly consider roughness except in an empirical or semiquantitative manner.* It was widely recognized that roughness could significantly decrease adhesion and thus have a great effect on friction, but on the level of a single asperity it was unclear how to factor this in. While this complication can generally be avoided at large length scales, where surfaces can be made almost arbitrarily smooth, at the nanometer scale the unavoidable atomic corrugation of even the smoothest surfaces was expected to have an effect similar to that of roughness. The applicability of these theories at this scale thus remained an unresolved question.

2.2 - Multi-Asperity Contact Mechanics

Roughness was much more the purview of the other major strand of development to come from Bowden and Tabor's work: multi-asperity theories of contact. Their explanation of friction in terms of the elastic deformation of a single asperity resulted in a sub-linear dependence of the friction force on load as a simple consequence of Hertzian contact mechanics. Some years later Archard demonstrated that the same mechanics applied to an asperity coated with microasperities which are in turn coated with still smaller microasperities does indeed yield successively closer approximations to the expected proportionality of F_{lat} and L.[12] He reasoned that the determining factor was whether an increase in load would merely increase the area of existing asperity contacts – resulting in a Hertzian $L^{2/3}$ dependence – or create new asperity contacts, thereby maintaining the average asperity contact area and giving a linear relation.

This basic analysis was further developed by Greenwood and Williamson (GW), who considered contact between a smooth plane and a nominally flat surface covered with a large number of spherically tipped asperities with randomly varying heights and identical radii of curvature.[13] Each of these asperities was assumed to deform according to Hertz contact mechanics, and the result for an exponential distribution of asperity heights was the proportionality of real contact area and load, recovering Amontons' laws. While Greenwood and Williamson granted that such a roughness distribution is not the best description of real

* This includes Tabor's work cited above. Though roughness entered into the physical justification for a transition parameter, his adhesive contact theory explicitly addressed only smooth surfaces.

surfaces, they maintained that it remains an effective approximation for the upper 25% of asperities on most surfaces. Furthermore, repeating this analysis with a more physical Gaussian distribution of asperity heights still returns an approximate proportionality between contact area and load. These results led them to propose that the origin of the laws of friction lay in the statistics of asperities. Numerous modifications and corrections to the GW multi-asperity theory followed, notable among them that of Bush and Gibson.[14,15] These authors also treated real surfaces in terms of a random spatial distribution of asperities, but the asperities were treated more realistically as paraboloids with variable radii of curvature. The asperity spatial, height and curvature distributions were determined by a random process model, and each asperity was assumed to deform as per Hertz contact mechanics. Though physically more precise, this model essentially reproduces the GW results: direct proportionality of real contact area and load at low loads and approximate proportionality in the other extreme.

The most significant recent development of multi-asperity contact theories was the work of Persson and co-workers.[16-18] Whereas all previous formulations had considered roughness on only one length scale, Persson's theory of contact mechanics allows for roughness on all length scales through the choice of an appropriate power spectral density. The theory is mathematically complex, but a fundamental result is that for surfaces with arbitrary random roughness the area of real contact is exactly proportional to the load, while the coefficient of friction is load-independent. This holds true for self-affine fractal surfaces as well in all but a few exceptional cases. For random and fractal surfaces, the resulting contact area is smaller than that previously calculated by multi-asperity contact theories by a factor of $2/\pi$. Other significant differences exist between Persson's results and those of the GW and BG theories, but these can be largely attributed to Persson's allowance of elastic coupling between nearby asperities through the bulk. Other authors, though, such as Manners and Greenwood, maintain that Persson underestimates the area in contact.[19] In re-deriving Persson's theory, in which roughness is gradually built up between two smooth surfaces consistent with certain boundary conditions, these authors noted that the spectral models used for such calculations inherently break down at atomic length scales if not even before, which demands the roughness be arbitrarily cut off. As with all other continuum-based multi-asperity theories, it is unclear down to which scale they can be considered valid.

2.3 - The Cobblestone Model

The theories presented thus far focused entirely on contact; it was uniformly assumed, as per Bowden and Tabor, that friction at the contact would be directly proportional to the contact area. With this consideration, it can be seen that the two strands of friction theory predict markedly different friction-load laws: in single asperity contact, F_{lat} is a clearly sublinear function of load, in most cases approximately $F_{lat} \sim L^{2/3}$; whereas multi-asperity contact yields exact proportionality in agreement with Amontons' laws.[*] These effects are often combined in practice in the cobblestone model, as for instance discussed by Berman *et al.*[20] Unlike the continuum theories above, this semi-empirical model explicitly allows for the atomic structure of surfaces and contacts – friction is interpreted as the work done against adhesive forces and the applied load when sliding two surfaces with interlocking asperities or atomic corrugation, which requires a slight vertical displacement. Berman *et al*. derive a linear friction-load law $F_{lat} = \mu L$ for the non-adhesive case without explicitly using the concept of contact area. However, the common observation of sublinearity and contact-area-dependence for macro- and microscopic adhesive contacts requires an additional term, yielding

$$F_{lat} = \tau A_{real} + \mu L \tag{5}$$

where A_{real} is an undefined but generally sublinear function of load and τ and μ are constants. At low

[*] This is strictly true only under the assumption of Bowden and Tabor friction, i.e. $F_{lat} = \tau A_{real}$.

loads the first term often dominates, and the system is said to be adhesion-controlled; at sufficiently high loads the second term dominates regardless of the strength of adhesive forces, resulting in friction as per Amontons' laws. While the separation of forces may be questionable at the nanoscale, where the interaction potentials of the interfacial atoms do not take such a simple form, this model has nevertheless proved versatile for fitting modern experimental data.

3 - Probing the Nature of Friction

The theories presented above were generally published with ample experimental support and motivated numerous inquiries into the microscopic nature of friction. A particularly useful and powerful tool in the long-standing controversy about adhesive single-asperity contact was the surface force apparatus, in which the deformation and adhesion of bent surfaces, primarily mica, glued onto crossed cylinders can be investigated even at sub-nanometer separation. In one characteristic study by Horn *et al.*[21], thin layers of silver were glued to glass cylinders and then coated with a molecularly smooth layer of mica. The cylinders were brought into contact with a controlled load, and the contact area and separation were monitored via interference of light between the two silver layers. Resolution of the separation with such a technique can be better than 2Å, but lateral resolution is limited to several μm. It was found that in concentrated salt solution, in which the dielectric constant is high enough to screen out any adhesive interactions at contact, the deformation profiles and contact area as a function of load fitted the Hertz theory excellently. In non-polar nitrogen gas, on the other hand, in which adhesive interactions can be expected to be much stronger, the cylinders were found to deform in accordance with the JKR theory. Furthermore, at pull-off the mica surfaces were observed to have a finite contact area, as predicted. Similar references may be found in the original papers discussed above, but because of their inability to probe properties on the nanoscale, these methods are outside the scope of this paper.

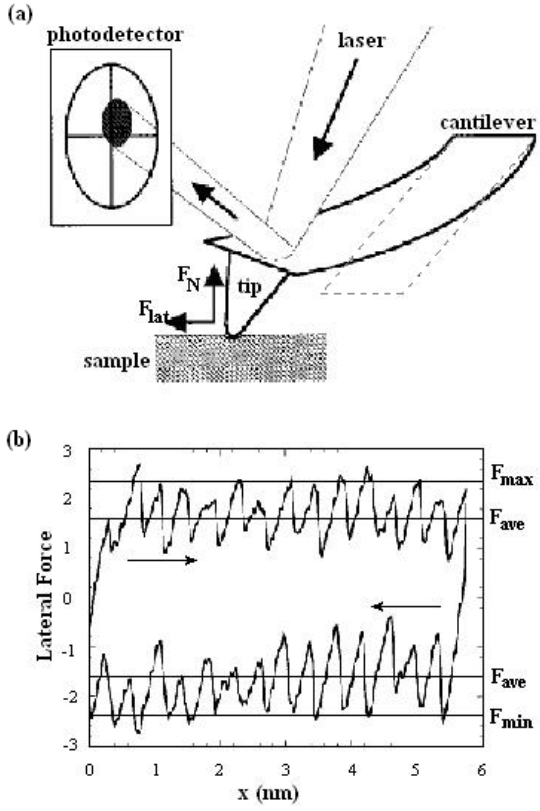

Figure 4. Basic principles of FFM. (a) A schematic of the AFM showing the torsion of the cantilever due to lateral friction forces and the detection thereof via deflection of the laser incident at the quadrant photodiode. (b) A typical example of stick-slip motion – torsion of the cantilever increases until the elastic force exceeds the static friction holding the tip in place, and it quickly slips to a new location. The periodicity of the peaks is directly related to the crystal structure of the surface. The area within the loop is equal to the energy dissipated through friction, and the average frictional force is related to the average separation of the upper and lower traces. Arrows indicate the sliding direction, and forces are given in arbitrary units. Adapted from (22)

Much more momentous for the field of nanotribology was the development in the early 1990's of the atomic force microscope (AFM) and in particular the technique of friction force microscopy (FFM). The AFM tip was and continues to be seen as the closest physical analogue of the single asperity that has played such a central role in friction theories, and it was quickly realized that FFM offered the potential to probe the

validity of single-asperity contact models of friction and investigate the influence of the atomic nature of matter. Before turning to experimental results, however, it is necessary to briefly review some of the general difficulties faced in FFM. In this technique the AFM tip is placed in contact with a surface and a controlled load is applied, as monitored by vertical cantilever deflection. When the tip is then displaced laterally, friction at the interface causes the tip to drag behind or stick, resulting in torsion of the cantilever (see Figure 4b). The vertical and lateral bending of the cantilever is not observed directly, but rather through the deflection of a laser beam reflected off of the cantilever, as shown in Figure 4a. Already at this point quantitative FFM entails considerable complications. For accurate measurement, the detection laser must be aimed precisely above the AFM tip, which is extremely difficult to achieve in practice, yet even slight shifts in the beam spot can greatly alter the friction coefficient observed at the same location on the same sample, as shown by Schwarz *et al.*[23]

Equally critical to quantitative data analysis is calibration for accurate calibration of the quadrant photodiode voltage output into lateral force measurements. Detailed procedures can be found in the literature;[23,24] the salient point is that this process unavoidably entails assumptions about the tip and cantilever geometry and elastic properties. Lateral forces, the most important for FFM, are particularly difficult to determine in standard systems as they involve cantilever twisting instead of simple bending – the corresponding calculations require further assumptions about the tip and cantilever properties. More important yet is the characterization of AFM tips, which represent half of the interface studied under FFM. Though commonly assumed to be ideal single asperities, AFM tips generally have unwanted Ångstrom-scale and larger protrusions which can disproportionately affect contact behavior. If FFM is to be used to investigate friction on the nanoscale and probe the influence of the atomic nature of matter, then the surfaces involved should be well characterized on the same scale or smaller. As the theoretical review above should have made clear, the degree of roughness is one of the determining factors in whether an interface falls under the single-asperity or multi-asperity regime, each with markedly different frictional properties. Most common methods, such as TEM and scanning a surface with known asperities, can only roughly characterize the tip surface, which cannot but limit the utility of FFM to conclusively test single- and multi-asperity theories of friction.

3.1 - Contact Area in FFM

Because of the pivotal role of contact area in the dominant theories of friction, an investigation of the interrelation of A_{real}, L and F_{lat} would be a logical starting point for the experimental study of friction on the nanoscale. However, the AFM produces data about frictional force as a function of normal load – contact area is not and generally cannot be measured. Because of the perceived importance contact area, many early efforts sought indirect methods to characterize it, one of the most commonly used being the measurement of lateral contact stiffness described by Carpick, Ogletree and Salmeron.[25] Contact stiffness is the force per unit displacement required to deform an elastic contact in a given direction, in essence the 'spring constant' of a contact, and by assuming a paraboloid-plane geometry for the AFM contact, it can be shown for small lateral displacements that the lateral contact stiffness is given by

$$k_{contact} = 8a\left[\frac{2-\nu_1}{G_1}+\frac{2-\nu_2}{G_2}\right]^{-1} = 8aG^* \qquad (6)$$

where G_1 and G_2 are the tip and sample shear moduli and a is the contact radius. The critical aspect here is that lateral contact stiffness is independent of both the tip radius of curvature and the model used to describe the tip deformation. It can be measured by slightly varying the lateral position x of the cantilever. As long as no slip occurs and the cantilever compliance is known, $k_{contact}$ can be determined from

$$\frac{dF_{lat}}{dx} = k_{total} = \left[\frac{1}{k_{contact}} + \frac{1}{k_{lever}} \right]^{-1} \tag{7}$$

This technique entails certain approximations about the system, including tip-sample geometry, tip rigidity, the non-interaction of lateral and normal forces and, critically, the absence of slip, a process particularly poorly understood on the nanoscale.

One excellent example of the use of lateral contact stiffness is the study by Lantz *et al.*[26] of the friction between Si AFM tips (12nm and 45nm) and freshly cleaved, atomically smooth $NbSe_2$ terraces in UHV. The contact stiffness was measured for a range of applied loads, and the corresponding contact radius vs. normal load data was fitted well with the M-D model[*], albeit with significant noise. Further measurements at higher loads in the stick-slip regime showed a reduction in noise, and the dependence of friction on normal load was distinctly nonlinear; these data showed even better agreement with the M-D model. This allowed the authors to conclude that friction is proportional to contact area even on the nanoscale, with continuum mechanics contact models thus applicable down to contact radii of 1-2nm.

Another landmark study sought to quantify the tip-sample contact area via electrical conductivity measurements. Enachescu *et al.*[27] examined the friction between 100nm tungsten carbide tips and a hydrogen-passivated diamond surface in UHV. Because of the hardness and inertness of these materials, this system was considered an ideal test case for the DMT theory on the nanoscale. In order to independently determine the load dependence of contact area, the diamond was doped with boron, enabling a measurement of the contact conductivity – because of the limited size of the contact, it was assumed that the conductivity would be proportional to A_{real} such that variation in current at constant voltage could be equated to variation in A_{real}. This same technique had been applied by Bowden and Tabor to macroscopic contacts to develop their original theory, but the validity of this assumption at the nanoscale is questionable. Still, the resultant current-load plots at constant voltage could be fitted well by $A_{real} \propto (L + F_{ad})^{2/3}$, which was interpreted as unambiguous confirmation that the load dependence of contact area in this system could be described by the DMT model (see Figure 5). Using a softer cantilever to increase sensitivity and remain within the wearless friction regime, the authors were able to find a reasonable DMT fit to the friction vs. load data for the small range of forces used. Unfortunately, friction data at loads near the pull-off force was unavailable as the motion of the cantilever consistently led to premature pull-off, a common problem in FFM. Nonetheless, a DMT fit using the shear strength and surface energy as free parameters was able to precisely recover the measured pull-off force. Once again, the fit of a single-asperity contact mechanics model to friction-load data and current-load data was taken to demonstrate that $F_{lat} = \tau A_{real}$ down to the nanoscale, at least for low forces.

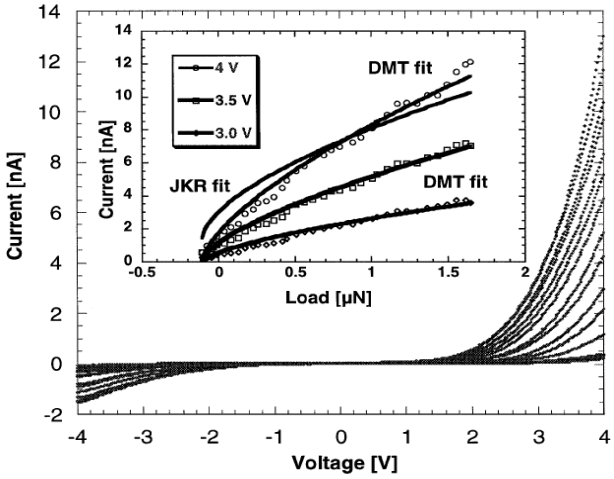

Figure 5. The variation of contact conductivity and area with load. I-V traces were collected for 128 different loads up to 1.7μN. Inset: the current-load plots at constant voltage, showing the excellent fit to the DMT model and the inapplicability of the JKR model. From (27)

[*] In this and all studies presented below, single-asperity contact models are interpreted as predictions of friction behavior by assuming the proportionality of contact area and friction.

As demonstrated by Schwarz *et al.*,[28,29] the contact area problem can also be addressed through rigorous control of the surfaces involved. Rather than measure the contact area itself, the authors relied on special tip manufacturing conditions to prepare and characterize tips of exact spherical geometry, and they restricted friction measurements to surfaces free of steps – in these strict conditions, it was found that the mathematical models of continuum mechanics could describe the data accurately even to the nanometer scale. Single-crystalline silicon AFM tips with typical radii of 5-15nm were coated with layers of amorphous carbon using electron beam deposition in UHV – the ionized carbon atoms were found to spread evenly on the surface due to coulomb repulsion, resulting in a smooth, well-defined spherical apex, and varying the deposition time could yield tip radii from 10 to 100nm. For a wide range of atomically smooth carbon surfaces, both in ambient conditions and under argon atmosphere, friction measurements with these tips could be fit excellently to a modified DMT force law $F_{lat} = \kappa(L + F_{ad})^{2/3}$, where κ is a generalized friction coefficient developed by the authors to take into account the radius of curvature of the tip and allow more direct comparison between systems. The conclusion from this data is that the DMT model is a valid description of sphere-plane contact in the regime of stiff materials and low adhesion, even at the nanoscale. However, it must be stressed that this was the case only for such rigorously prepared tips – AFM tips straight from the manufacturer gave load dependences from $L^{0.4}$ to $L^{1.2}$ and even the specially prepared tips no longer held to the $L^{2/3}$ law if they had the slightest deviation from spherical geometry, for instance due to wear. The results were not as unambiguous for mica and GeS surfaces, though these were also atomically smooth.[29] When cleaved in air both surfaces exhibited friction in reasonable agreement with the DMT model on average, but with much greater variability. In argon, their surface energy and reactivity proved so high as to make meaningful measurement impossible. However, GeS cleaved in air and measured in argon yielded a linear friction-load dependence, possibly caused by reactions between the tip and surface wearing the tip down into a multi-asperity contact. One clear result is that strict geometric controls are not necessarily sufficient to ensure single-asperity friction in the AFM – there must be more at work.

Indeed, studies of contact area alone cannot elucidate all of the important mechanisms of friction on this scale. This can better seen in another study by Schwarz *et al.*[30] which found contradictory data for GeS, a common occurrence in nanotribology. C_{60} was sublimated in UHV onto freshly cleaved, atomically smooth GeS and formed epitaxially layered islands. Measuring friction across the entire surface under ambient conditions showed a marked contrast between surface materials, with friction on the exposed GeS initially lower than on the C_{60} monolayers. Increasing the applied load led to a reversal of this contrast, demonstrating the different dependences of friction on load for these two materials. The friction vs. load data was fitted to a generalized DMT model of the form $F_{lat} = k(L + F_{ad})^m$, and it was found that the interaction of C_{60} with the tip showed perfect Hertzian contact, i.e. $m = .666 \pm .017$, whereas GeS exhibited very nearly linear behavior with $m = .891 \pm .02$. This is a significant departure from the DMT fit for GeS found above. More importantly, the simultaneous observation of perfect DMT friction on C_{60} calls into question the proposal that the linear or nearly-linear friction-load law is due to the multi-asperity nature of the contact and clearly indicates that additional factors are involved.

3.2 - The Effect of Tip Geometry

A great many other nanotribological studies have focused on the elucidation of these other factors affecting friction in the AFM rather than on the direct relation between contact area, load and friction, due in large part to the evident complexity of reliably characterizing the contact. For instance, one study by Carpick *et al.*[31] attempted to quantify the role of tip profile by using the common technique of tip blunting

under high loads. A platinum-coated silicon nitride AFM tip was roughly characterized by scanning a surface with sharp, known features; it was shown to be essentially parabolic, with a radius of 140nm. The friction between this tip and freshly cleaved mica was investigated in UHV, yielding an excellent fit to the JKR model, including finite friction at zero applied load and at pull-off. The tip was then deliberately flattened and friction data were again collected. The flattened tip exhibited lower friction under positive load and higher friction under negative load than would be expected for a parabolic JKR-model tip with that zero-load contact area and pull-off force and generally fit the JKR model quite poorly. However, this behavior proved to be very well described by a higher-order "extended JKR" model developed for tips with height profile $z = cr^n$. Specifically, it fit the model for $n = 6$, and subsequent measurement of the tip shape revealed it to conform closely to an r^6 profile. While this result does not contain much predictive power, it does serve to highlight the important role of tip shape and the characterization thereof in FFM. Furthermore, when the effects of shape can be accounted for, tip blunting presents a quick, simple method to check for the contact area dependence of observations in the AFM.

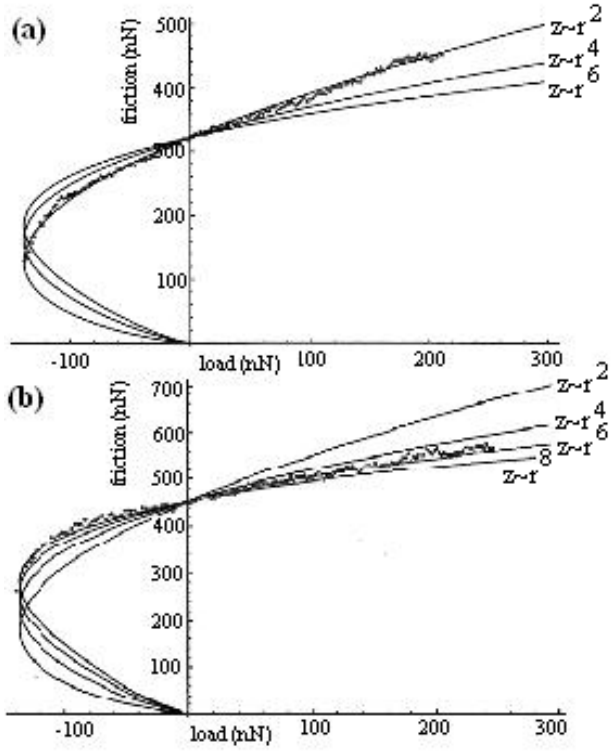

Figure 6. The effect of tip blunting. The friction versus load data for an AFM tip (a) before and (b) after blunting. Solid lines show the JKR or extended JKR model prediction for a tip with the height profile given at right. From (31)

3.3 - Adhesion Control in FFM

Other investigations have focused on the role of adhesion in FFM. Though the research cited thus far may not have made the point sufficiently clear, there have long been many competing observations of the dependence of friction on load at low loads. At higher loads, outside the regime of wearless friction, observations are more uniformly in agreement with Amontons' laws. This is often described by the cobblestone model (Eq. 5), in which load and adhesion contributions to friction are explicitly separated:

$$F_{lat} = \tau A_{real} + \mu L$$

Because only the first, sublinear term is dependent on adhesion, it should be possible to reduce its effect through control of adhesion. A recent study by Colburn and Leggett[32] of the role of adhesion in friction on the nanoscale proved particularly compelling. They demonstrated that it is possible to control friction behavior through solvent environment and surface chemistry. They measured the friction in ethanol and perfluorodecalin (PFD) between surfaces coated with self-assembled monolayers (SAMs) of polar or non-polar thiols and unfunctionalized or thiol-functionalized silicon nitride tips. The friction versus load data were analyzed with the M-D model using the transition parameter α defined by Schwarz (Eq. 4). In non-polar PFD, it was found that 'like' tip interactions, i.e. polar tips on polar surface, led to excellent JKR behavior, while 'unlike' interactions resulted in a good DMT fit. The mildly polar silicon nitride tips yielded an intermediate, near-JKR value of α on the polar surface and a good DMT fit on the non-polar surface. In ethanol, on the other hand, friction clearly varied linearly for all tip-surface combinations.

Treating adhesion as primarily an effect of van der Waals attraction, the authors proposed that single asperity contact mechanics can generally be observed in non-polar media, where dispersion forces and other attractive interactions can cause great enough adhesion to affect contact and friction is primarily adhesion-controlled. In polar liquids, these interactions are weak enough that the system becomes load-controlled. Another interesting consequence of these results is that tip chemistry had a much greater effect on frictional behavior than tip size, which led to the conclusion that the fundamental quantity in friction is not contact area but the number of bonds made and broken across an interface.

3.4 - Environmental Effects in FFM

Additionally, the role of solvent and ambient environment has been observed to extend beyond control of adhesion. For instance, the composite-tip model of Putman *et al.*[33] proposes that the relative vapor pressure of water and other contaminants can cause switching between single- and multi-asperity behavior. The friction between long, narrow silicon nitride tips and mica was measured in ambient conditions, revealing a decidedly sublinear dependence of friction on load as per single-asperity contact mechanics. When the AFM chamber was evacuated and filled with nitrogen gas, the friction varied linearly with load. The same results were achieved on a glass surface tested first in ambient conditions and then in argon after evacuation. Indeed, both ambient measurements gave excellent fits to $L^{2/3}$, while the gas data appeared perfectly linear. The proposed explanation of this phenomenon hinges on the small-scale multi-asperity nature, i.e. the atomic roughness, of standard AFM tips. In ambient conditions, every surface is covered by a monolayer of water and other contaminants, which due to meniscus forces will more or less fill in the nanoscale roughness of the tip, making it relatively spherical so that the total system behaves as a single asperity. Evacuation removes a significant proportion of these contaminants, and after flooding with gas the relative vapor pressure is too low for sufficient meniscus curvature and many of the crevasses in the tip remain unfilled, resulting in a multi-asperity response. Other results could also support such a model; for instance Hu *et al.*[34] found variable sublinear power dependences for the friction of silicon nitride cantilevers on mica in air and water, but using ultrapure water to remove contaminants resulted in stronger friction directly proportional to load.

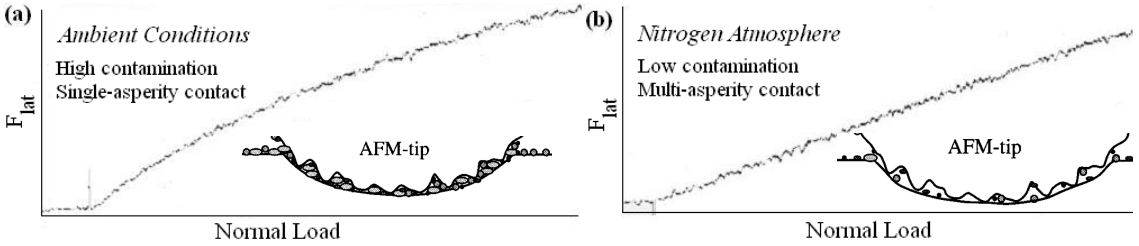

Figure 7. The composite-tip model. Raw AFM data for the friction of a silicon nitride tip on mica (a) in ambient conditions and (b) in nitrogen atmosphere after vacuum pumping, in arbitrary units. There is a clear transition from sublinear to linear friction. Insets: cartoon of the composite-tip model showing the proposed effect of contaminants on a rough tip. From (33)

3.5 - The Role of Crystal Structure

A final factor in FFM that merits special attention here is crystal structure. Unlike the experimental conditions described above, tip and surface crystal structure are rarely characterized in practice and are still more rarely under experimental control, yet the effects can nonetheless be profound. Some studies, such as that by Gao *et al.*[35], focus on the frictional behavior of different crystal faces. In this work, the friction between amorphous carbon tips and the (001) and (111) faces of microcrystalline diamond were measured in nitrogen. The data showed a modest, reproducible sublinear curvature at low loads and fit well to the M-D model, which allowed extraction of the work of adhesion, the friction coefficient and the Schwarz transition parameter α (Eq. 4). The work of adhesion, pull-off force and friction force were found to be markedly lower for the (111) versus the (001) face. The quality of the M-D fit must be treated

with caution, though, as the transition parameters extracted fell between 0.5 and 1, indicative of near-JKR behavior, while calculations of Tabor's parameter directly from realistic system quantities suggested that the DMT model would be much more appropriate. Nonetheless, the result that friction on the (111) face of diamond is lower than on the (001) face is unambiguous and particularly interesting in that it defies explanation by the continuum theories generally applied, all of which implicitly assume isotropic materials. Another interesting observation was the spatial variation of friction on the same crystallite – friction data and pull-off forces coincided almost completely for repeated measurements at the same location, but repeating the same measurements at different spots on the same crystallite yielded widely varying values. There was insufficient data to suggest a cause, but this is fairly clearly beyond the realm of current continuum friction theories; explaining such variation remains a key challenge in nanotribology.

The crystal structure of the bulk can also have a strong effect. For instance, Riedo *et al.*[36] measured the friction between a silicon tip and graphite, amorphous diamond-like carbon (DLC) with controlled proportions of sp^3-hybridization and carbon nitride (CN_x) with controlled proportions of nitrogen. There was in fact no observable variation in frictional behavior for different degrees of sp^3 hybridization or nitrogen content, but there was clear variation between materials for the same tip: graphite and CN_x yielded a linear relationship between friction and load, while the load dependence on DLC was clearly sublinear. Moreover, it was found that friction on DLC was greater than on CN_x, which was in turn greater than on graphite, while adhesion followed precisely the opposite trend. The low friction of graphite is easily explained in terms of the low shear strength of the graphite layers, but the difference between DLC and CN_x is less apparent. One proposal was the influence of surface morphology, as the CN_x film was much rougher than the DLC. However, a simultaneous measurement of friction and topology showed no correlation between local friction and even large (2nm) features, indicating the mechanism must lie elsewhere. The data from this experiment were insufficient to shed light on this, and the sensitivity of the AFM to extraneous factors may mean this question would be better addressed in simulations, but again current continuum friction models appear inadequate to explain this phenomenon.

This brief presentation of experimental results should have made clear the versatility and inherent limitations of friction studies with the AFM. Indeed, most of the theories of friction discussed above were initially published with the caveat that continuum-based contact mechanics should break down at small length scales where the atomic nature of matter becomes significant. It was hoped that FFM could be used to investigate the limits of validity of continuum-based friction ideas at small length scales, but the results were hardly unambiguous. Great variability in the load dependence of friction has been observed, with different interfaces yielding excellent DMT, JKR, M-D or linear fits; nor has it been uncommon for different groups to produce seemingly contradictory friction results for the same interface, or to observe inexplicably large spatial variation in the friction between the same AFM tip and crystal surface. A major contributor to these difficulties is the high sensitivity of the AFM – as briefly outlined above, carefully controlled experiments can clarify the influence of additional factors such as chemical environment, tip shape and crystallographic orientation, but these are not always under experimental control. A still more serious limitation to the utility of the AFM for probing the range of validity of continuum-based friction is the inability to directly characterize contact area, a quantity central to all of the theories above. It can at best be measured indirectly through conductance or derived quantities like contact stiffness, but these entail numerous assumptions and approximations of their own. Obstacles such as these demand that the question be approached with different techniques as well, and the rapid growth of computational power in the past decade has led to the development of molecular dynamics (MD) simulations as a valuable tool for the investigation of the laws and mechanisms of friction on the nanoscale.

4 - Atomistic Simulations of Friction

Before addressing the key results of nanotribological simulations, it is worth reviewing some of the common techniques employed and limitations encountered. These can perhaps be best seen in tandem AFM-MD studies of the same system, for instance in two related diamond-on-diamond friction studies by Gao *et al.*[35] and Brukman *et al.*[37] One of the obvious objectives of nanotribological simulations is to accurately model the key interactions and realistic experimental conditions to achieve reasonable agreement with experiment– this is essential for the extraction of useful, quantitative physical data from AFM results. For this reason most studies of this sort have been limited to systems that are amenable to replicable AFM measurements and accurate modeling, and foremost among these is hydrogen-passivated diamond, which the second-generation reactive empirical bond-order potential (REBO)[38,39] is known to describe especially well. The potential includes no van der Waals interactions, though; these are taken into account in the adaptive intermolecular REBO (AIREBO).[40] Unfortunately, the AIREBO potential is much more computationally demanding and thus often used only to demonstrate that the inclusion of adhesion results in no qualitative changes in the data beyond a dampening of individual atomic fluctuations, a widespread but not uniform result found in both (35) and (37).

Similar computational compromises characterize many of conditions set in MD simulations, most notably regarding tip properties and substrate size. Thus in the diamond-on-diamond studies the authors simulated an approximately hemispherical tip with a radius of only ~15Å; these were "carved" out of a single crystallite of diamond so as to be stepped and incommensurate in all sliding directions with the diamond (001) and (111) faces under consideration and fully passivated with hydrogen. This tip was assumed to be fully rigid, a common simplification that lends itself best to diamond and similar systems. By way of contrast, the actual AFM tips were made from amorphous diamond, were more than an order of magnitude larger and were not fully passivated. The simulated diamond surfaces also reflected significant compromise – they extended only several tip diameters in each lateral direction before periodic boundary conditions were assumed and consisted of 13 layers of carbon atoms, of which only the uppermost were unconstrained. The most significant deviation from experimental conditions regards the sliding speed of the simulated probe – even the most cutting-edge simulations must use sliding speeds 6 or 7 orders of magnitude above those achieved in the AFM. The influence of sliding speed on friction is in itself an important branch of tribological study, so this is certain to have an effect on the data produced, albeit one difficult to quantify. Likewise, MD simulation results are known to depend on the tip and sample size, with much greater fluctuations in individual atomic contributions, and thus less reliable averages, for small simulations. Nevertheless, even in the face of these limitations MD simulations can prove useful at this level, particularly in concert with AFM data.

The agreement between simulations and experiment in (35) and (37) is admittedly not great – whereas the AFM data could be fit well by the DMT model and showed modest but reproducible curvature in the low-load regime, the MD simulations returned a linear friction-load law. Other simulations in the literature also indicate that amorphous AFM tips should disagree sharply with single-asperity contact mechanics predictions, as their greater disorder and atomic-scale roughness are thought to mimic the effects of multi-asperity surfaces. The authors suggest that unavoidable trace contamination could counterbalance this effect to give the unexpected single-asperity result, akin to the composite-tip model. In spite of this discrepancy, the magnitudes of measured and simulated forces were in reasonable agreement, as were the general trends for temperature dependence and sliding direction. This enabled crucial insight into the

mechanism of the crystallographic face- and direction-dependence of atomic friction on diamond in terms of the surface C-H bonds the tip encounters and the corresponding pathways for energy dissipation available. In combination and agreement with AFM data, then, MD simulations can be extremely useful for elucidating the mechanisms and nature of friction on the nanoscale. Because of the sensitivity of the AFM to so many factors, not all of them under strict experimental control (in this instance trace water and adsorbed particles), disagreement cannot necessarily be taken as an invalidation of the simulation model used, but rather an indication that the simulation has not sufficiently considered all relevant experimental conditions. This often ambiguous relationship between experiment and simulation should be borne in mind through the following discussion of significant simulation results.

4.1 - Atomistic Friction and Surface Morphology

A most fruitful focus of nanotribological MD simulations has been the role of crystal morphology in friction, i.e. the effect of commensurate, incommensurate, amorphous and stepped interfaces. The basic picture of atomistic friction in MD simulations is that of surface molecules* settling into an equilibrium determined by a balance between interactions within the surface and across the interface; friction reflects the net resistance of all such molecules to being moved out of their equilibrium positions. When the interfacial interactions are much stronger than interactions within the bulk, all surface molecules should be able to simultaneously reach a free energy minimum, with a correspondingly large resistance to displacement. In the other extreme, where surface molecules are not as free to rearrange in response to the interfacial potential, surface morphological factors are expected to come into play. In commensurate interfaces, surface molecules are able to simultaneously lock into registry and are displaced into and out of this local free energy minimum entirely in phase, an effect experienced as friction. Surface molecules in incommensurate interfaces, on the other hand, effectively sample all locations in the interaction potential environment at once, with the result that the surface experiences no net change in the potential upon displacement – just as many atoms resist lateral motion as support it, resulting in a frictionless interface. Known as superlubricity, this has been experimentally observed, for instance, on graphite[41].

More intriguing for understanding the fundamental mechanisms of friction on the nanoscale, though, is the rarity of this phenomenon. Indeed, the concept above suggests that almost no two solids in contact should exhibit friction, save in the rare occurrence of naturally commensurate surfaces and sliding directions or interfacial interactions strong enough to force commensurability. This is clearly not the case, and early investigations of this discrepancy focused on the role of "third bodies"† confined in the interface, which it was proposed could access a range of metastable states allowing them to enter into simultaneous registry with both surfaces – each surface then interacts with an effectively commensurate surface, with sliding friction as the result.[42] The initial molecular dynamics studies of this effect by He *et al.*[43] and He and Robbins[44] used flat,

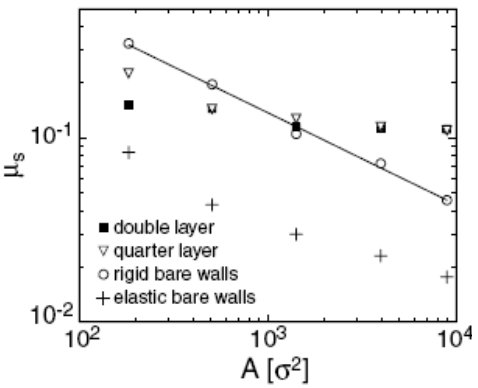

Figure 8. The effect of adsorbed molecules. Simulated friction coefficient is displayed as a function of constant contact area without (circles and crosses) and with (squares and triangles) adsorbed molecules. The same constant friction coefficient is quickly reached for a wide range of adsorbate coverages (only 2 shown). The solid line is a fit to $\mu_s \sim A_{real}^{-1/2}$. From (45)

* The term 'surface molecules' shall be taken here to also include surface atoms in the limit of uncontaminated crystalline surfaces.

† These third bodies are similar to the generally unavoidable contaminants discussed in the composite-tip model, such as water, adsorbed hydrocarbons and small airborne molecules.

smooth crystalline surfaces, which quenched any possible contact area dependence. Both simulations found linear friction for the bare commensurate interface and vanishing friction for bare incommensurate interfaces, while the linear relation of Amontons' laws was uniformly recovered in the presence of intermediate adsorbed molecules. Subsequent simulations by Müser *et al.*[45] of flat interfaces with different contact areas provided further support for this concept (Figure 8). Such results led to the interpretation of the role of adsorbed molecules as mobile hard-sphere "cobbles" in a modified cobblestone model. Because of the great difficulty of avoiding such contamination in typical experimental conditions, this could be an adequate explanation of the ubiquity of friction regardless of apparent incommensurability, though the restriction of these simulations to flat surfaces makes a direct application to AFM data difficult.

This work of Müser *et al.* yielded insight into the friction behavior of bare surfaces, as well. Using a greatly simplified potential to model repulsion between two flat but rough surfaces[*], the authors found an analytical expression for a nominally load-independent friction coefficient:

$$\mu \approx \max_{x_t} \left[\frac{1}{\xi} \sum_k i k_x \delta\zeta_b(k) \delta\zeta_t^*(k) e^{ik \cdot x_t} \right] \tag{8}$$

where ξ is the length scale of the interaction and the $\delta\zeta(k)$ are Fourier transforms of the bottom and top surface height distributions. It follows directly from this expression that commensurate crystalline surfaces, which share a common periodicity in their height distributions and thus correlated Bragg peaks in the Fourier transforms, will exhibit sliding friction independent of contact area and thus linear with applied load. Infinite incommensurate contacts will by the same reasoning have a vanishing friction coefficient, though in finite systems contributions at the edge lead to small values of μ. The Fourier transforms of nominally smooth but disordered surfaces will have many overlapping rings of diffuse scattering, and in the specific instance of area-independent corrugation this leads to $\mu \sim A_{real}^{-1/2}$. As can be seen in Figure 8 above, this prediction was confirmed in simulations for both rigid and compliant surfaces.

This result was used in an influential work by Wenning and Müser[46] to make one of the first connections between such simulations and FFM results. Indeed, the relation $\mu \sim A_{real}^{-1/2}$ for smooth but disordered surfaces allows an almost trivial explanation of the common observation of single-asperity contact behavior in the AFM. Assuming non-adhesive Hertz contact mechanics ($A_{real} \sim L^{2/3}$) for simplicity, the result of Müser *et al.*[45] immediately returns the expected law $F_{lat} = \mu L \sim L^{2/3}$. Of course, the validity of assuming Hertzian contact mechanics remains in question, and Wenning and Müser investigated the issue with one of the first simulations of friction involving curved AFM tips and thus a contact area that varies with load. They simulated commensurate, incommensurate and amorphous tip morphologies. As expected from previous results, the friction on the commensurate tip was proportional to the applied load. The authors comment as well on the single-atomic data: individual atoms experienced widely varying local

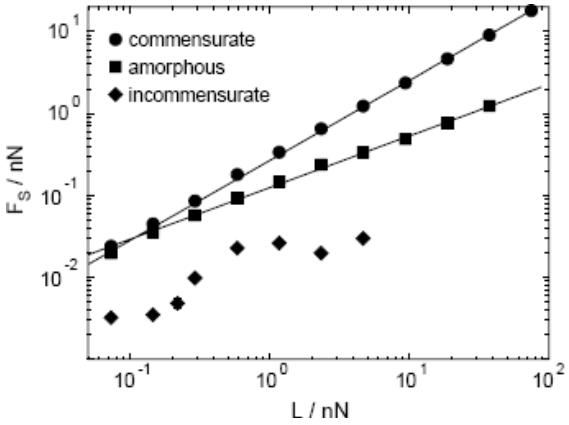

Figure 9. Simulated friction with curved AFM tips. The simulated friction-load data for commensurate, amorphous and incommensurate AFM tips. The commensurate data are fit to $F_s \sim L^{.97}$ and the amorphous data to $F_s \sim L^{.63}$. The incommensurate tip data could not be fit to any simple model. From (46)

[*] Numerical calculations with more realistic potentials resulted in the same qualitative trends presented here.

pressures and were thus deflected differently from their equilibrium positions. The resulting plot of atomic contributions to friction versus atomic load (not given) is said to show clear sublinearity. The linear friction behavior of the tip as a whole, then, is interpreted as a statistical effect akin to the GW multi-asperity contact theory.[13] The amorphous, i.e. smooth but disordered, tip also conformed to theoretical predictions, with a good fit to $F_{lat} \sim L^{0.63}$. As for the incommensurate tip, finite friction was observed with a strong dependence on the precise number of atoms in phase with the substrate. Though the dependence could not be quantified, this disagreement with previous work clearly indicates the significant role of tip curvature and variable contact area.

4.2 - The Breakdown of Continuum Mechanics?

The simulations cited above and similar early investigations firmly established tip and surface morphology as critical factors in determining the frictional behavior of nano-sized contacts, though the ubiquity of intervening third bodies made this difficult to evaluate experimentally. These concepts provided the foundation for numerous announcements of the breakdown of continuum mechanics descriptions of friction at the nanoscale. Notable among them is a study by Luan and Robbins focused specifically on contact mechanics and the deviations caused by atomic-scale surface roughness.[47] While many previous simulations had assumed that at small enough length scales two interacting surfaces could be treated as locally flat, Luan and Robbins sought to incorporate recent observations that surfaces tend to become steeper and more sharply curved at small length scales; it was not clear how continuum contact mechanics could be applied to such surfaces. To this end, crossed-cylinder and sphere-plane contact was simulated for the following morphologies: bent commensurate, bent incommensurate and stepped crystal and amorphous cut glass. All tips had realistic radii, ~30nm, but were made as smooth as consistent with their morphologies, with no deviations from the average surface beyond one atomic diameter. The authors concede that realistic AFM tips are generally much rougher, but roughness at this scale is rarely characterized in practice or explicitly considered in experimental analysis.

Interacting with a truncated (non-adhesive) L-J potential, all crossed cylinders and spherical tips showed close agreement with continuum mechanics predictions for indentation depth as a function of load, with the only discrepancy a slight uniform shift due to surface roughness causing earlier contact. The contact area data deviated much more from continuum models, indicating that continuum mechanics consistently underestimates the area of AFM contacts. This is particularly significant at low load, where the error is close to 100%; still, the functional dependence approximately matches the $L^{2/3}$ prediction of non-adhesive Hertz theory, and a better fit to the simulation data can once again be achieved by adding a constant (though tip size-dependent) correction. Indeed, the insufficiency of continuum models is not fully apparent until a consideration of local parameters such as the pressure distribution. Both bent surfaces correspond quite well with continuum predictions except at the very edges of the contact (an effect of underestimating the contact area), but the amorphous surface showed extreme fluctuations comparable with the mean pressure, even after averaging over the length of the cylinder. The data for the stepped morphology show essentially no relation to the continuum model applied, with lower pressure in the inner regions of each terrace and sharp pressure peaks at each edge. As seen in Figure 10, similar results were obtained with spherical tips. The results for these last two morphologies are especially significant as most AFM tips are expected to fall under one of these categories. However, it must be pointed out that while the stepped data differ greatly from continuum predictions for a parabolic tip, the qualitative match with continuum predictions for a flat punch is excellent. A reasonable conclusion, then, is that precise characterization of the atomic-scale surface roughness could extend the applicability of continuum models to still smaller contacts by informing the choice of an appropriate model.

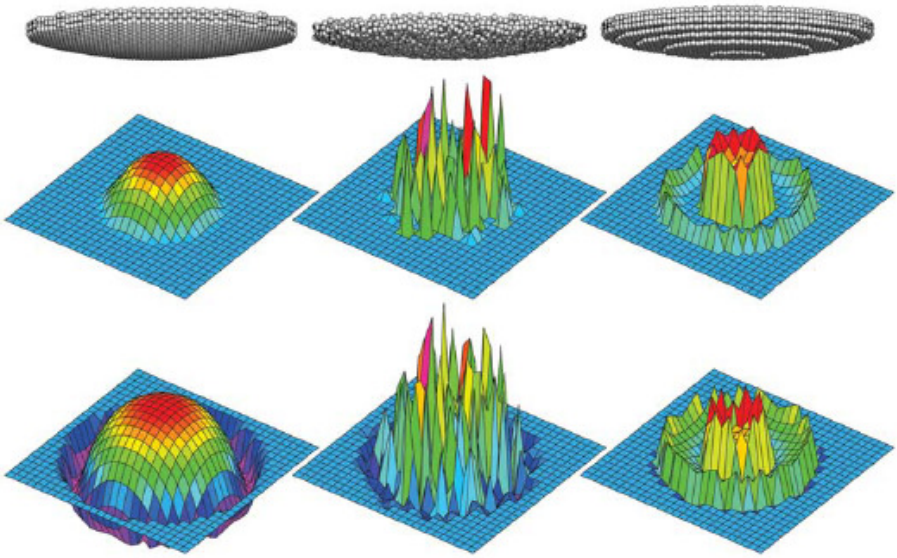

Figure 10. Local pressure and tip morphology. The local pressure distribution for the central region of each tip (bent crystalline, amorphous and stepped) is plotted both in the absence (above) and presence (below) of adhesion. From (47)

A similarly strong dependence on morphology was evident in the friction simulations. The amorphous and especially the incommensurate surface showed much lower friction in general, presumably because of the inability of tip atoms to enter registry with the substrate. The amorphous case is particularly interesting, as the friction appears proportional to the applied load. Referring again to the atomic pressure distribution Figure 10, it would be reasonable to interpret the amorphous tip in terms of an atomic-scale multi-asperity contact, which has been shown to lead naturally to a linear friction law[13,16]: yet another indication that continuum mechanics friction theories can be applied to friction on the nanoscale with appropriate care. The clearly sublinear friction data for commensurate and stepped surfaces also yield a curious result: while the friction is not found to vary linearly with the real contact area found in the simulation, a surprisingly accurate qualitative fit is attained using $F_{lat} = \tau A$ with the 'incorrect' continuum mechanics contact area. Though the authors refrain from discussing the implications of this, it is a particularly important point which merits further discussion below.

An overview of the key results from a subsequent, more quantitative study by the same authors is also in order.[48] This work is distinguished by the additional factors included in the model to better approximate ideal experimental conditions (such as a numerically determined anisotropic elastic modulus and a drastically thicker substrate of 150 atomic layers). Contact was simulated between rigid spherical tips and an elastic substrate, with the tips divided into amorphous, stepped[*] and bent crystalline (commensurate and incommensurate) and given minimal atomic-scale roughness. General trends for non-adhesive contact were similar to those presented in (47), with good Hertzian fits for the results for commensurate surfaces and extreme variations in the single-atomic data for amorphous and incommensurate surfaces. It must be stressed, however, that averaging these data out over rings of atomic thickness returned behavior in reasonable agreement with the Hertz prediction until the contact edge, which has already been established to be underestimated in continuum theories.

[*] The results for stepped tips were again in accord with continuum predictions for a flat punch rather than a spherical tip and revealed no new behavior in this regard.

One last notable result in the non-adhesive regime regards contact stiffness, which had rarely been addressed in other simulations. Luan and Robbins found that the simulated contact stiffness data were drastically lower than the continuum predictions, in some cases by an order of magnitude, and an analysis of the atomic data revealed the cause to be compliance at the interface. In the definition of contact stiffness used widely with single-asperity theory and in FFM, the atoms at the interface are assumed to remain fixed, but this is unrealistic and unjustifiable. Allowing some degree of atomic slip in the determination of contact stiffness, in terms of an interfacial stiffness k_i, does in fact return values for the remaining contact stiffness in close agreement with the Hertz theory. This already calls some of the experimental results derived from contact stiffness into question. And further caution is in order when working with contact stiffness even after taking interfacial compliance into account. From the continuum mechanics definitions of lateral contact stiffness as $k_{contact} = 8G^*a$ and friction force as $F_{lat} = \tau A = \tau a^2$, the ratio $F_{lat}/k_{contact}^2$ should be independent of load. At higher loads, this ratio was found to be approximately constant for all morphologies in the simulation, though the stepped surface in particular behaved in no way like a paraboloid single asperity. The fitting of such derived quantities in an experiment thus need not imply anything conclusive about the contact area behavior.

The subsequent simulation of adhesive contact is unique for producing a non-trivial change in contact and friction behavior, requiring a fit to the more complicated M-D model instead of a simple Hertz-plus-offset picture. Using data for the work of adhesion, radius of curvature and effective elastic modulus measured from other simulations, Luan and Robbins encountered great difficulty in simultaneously fitting the pull-off force and contact radius data, particularly when longer-range interactions were allowed.* Fits by the M-D model at intermediate points were even worse – the Dugdale potential assumes constant adhesion throughout an annulus between radii a and c, but the pressure distribution returned by the simulation unsurprisingly contained smoothly varying curves with no sharp onset of surface separation (Figure 11). Nonetheless, when compared to the bent commensurate results the data in the adhesive regime follows similar trends as described above for non-adhesive data versus the continuum Hertz model. Furthermore, data for the location of maximum adhesive force follows the trends of the JKR model closely, just as the locations of the crossover from repulsive to attractive interactions and the outer edge of the contact region follow predictions of the M-D model; the only necessary correction is again a uniform increase by several atomic diameters, with the biggest correction for amorphous tips.

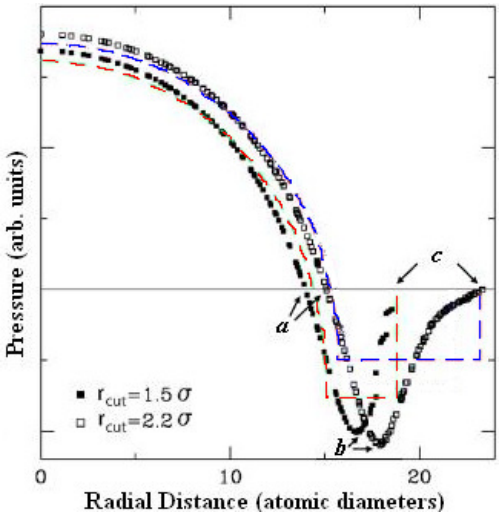

Figure 11. Pressure distributions under adhesion. The simulated local pressure plotted as a function of radial distance for two different L-J potential cut-off radii. Dashed lines are fits to the M-D model. Radii a, b, and c correspond to the edge of repulsive interactions, the maximal attractive interaction and the edge of the contact zone, respectively. Note the poor fit in the annulus a to c. Adapted from (48)

In reviewing the results of Luan and Robbins, one cannot but wonder if announcements of the breakdown of continuum mechanics at the nanoscale are not premature. Out of the vast body of simulations they

* The authors stress that the M-D model is sufficiently flexible that all of the data produced could be fit excellently if these three parameters were freely adjustable. The scale of adjustments required proved to be on par with typical experimental uncertainties for these properties, highlighting the difficulty of testing continuum theories with the AFM even when contact radius and other quantities can be accurately measured.

considered, all but a few results followed trends that spring directly from continuum contact mechanics theories, albeit not necessarily the trends that would have been selected without a detailed knowledge of the morphology and atomic roughness of the surfaces in question. And that may be the crux of the matter – single-asperity contact theories in most cases fail due to atomic-scale roughness, but these theories were formulated for smooth elastic solids, with no quantitative mechanisms to take roughness at any scale into account. Molecular dynamics simulations, on the other hand, are able to account for roughness, interfacial compliance and other effects that are not included in the most familiar models. What simulations such as these may actually break down is the use of inapplicable contact mechanical models, as exemplified by the poor fits to the M-D model by adhesive simulation data in (48). Granted, the pressure distribution differs significantly from the constant-adhesion annulus assumed by Maugis, but that was not originally intended to be applied as a physical potential. Rather, it was introduced by Maugis as a mathematical convenience to avoid self-consistent calculations and recover reasonable data for the work of adhesion and contact radii.[9] To expect more detailed agreement than these basic parameters is simply not reasonable, the more so for rough interfaces.

One final noteworthy result of Luan and Robbins pertains to the persistent question of contact area. For amorphous and bent crystalline tips, in both the adhesive and non-adhesive regimes, with one exception they observed a linear relationship between friction force and the square of any radius determined in their simulations. This is noteworthy both for returning a fundamental assumption of continuum mechanical friction theory, one which had been called into question by earlier simulations, and for the case of the exception. In (48) the bent commensurate tip with non-adhesive interactions was found to experience friction proportional to the applied load, while contact area scaled according to the Hertz model $A \sim L^{2/3}$. In (47), on the other hand, the same tip-substrate system had a real contact area slightly larger than the Hertz prediction and a clearly sublinear friction law that scaled well with the incorrect continuum mechanical contact area. It is contradictions of this sort that motivated one of the most recent studies to herald the breakdown of continuum mechanics at the nanoscale.[49] The authors maintain that contact area is consistently determined incorrectly in the literature and propose an alternative method: counting the number of atoms in contact across the interface[*] and multiplying by the average surface area per atom.

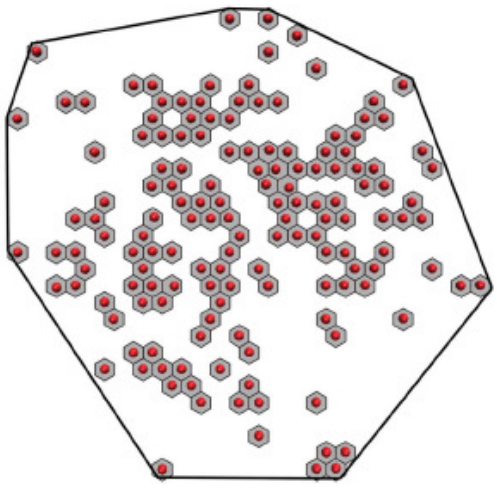

Figure 12. Contact area definitions. Circles indicate atoms considered in contact, with hexagons showing the average area assigned to each. The real contact area is defined as the sum of all hexagons. The asperity contact area is defined as the entire region inside the outer polygon. From (49)

To test the interrelation of friction, contact area and load in terms of this definition, Mo *et al.*[49] simulated the friction of a 30nm hydrogen-terminated DLC tip on a hydrogen-terminated diamond (111) surface. Most simulation conditions used are standard – sample and tip thickness, REBO potential, sliding speeds – but to more accurately model contact behavior the authors allowed the tip to deform together with the surface. Under these conditions, it was found that the asperity contact area (see Figure 12) scaled almost in accordance with the non-adhesive Hertz theory, giving $A_{asp} \sim L^{0.7}$. Friction, however, was found to vary in direct proportion with the applied load, a seeming violation of one of the fundamental tenets of friction

[*] This is not defined in (49), but a standard practice in nanotribology simulations is to count any atoms within the potential cut-off radius of the other surface as in contact.

theories, i.e. $F_{lat} = \mu L \neq \tau A_{asp}$. This breakdown is explained in terms of the contact area: at the nanometer length scale, the standard definition of contact area is simply no longer sufficient. This is entirely reasonable – at the scale where atomic roughness becomes noticeable, only the most extended atoms, the effective asperities, will be in contact at low load, leaving little justification for including the potentially large, low-lying non-contacted atoms in the contact area. The usual law is in fact returned when the real contact area is redefined in terms of the number of atoms in contact, which is in turn directly proportional to the load. This is a hallmark of rough or multi-asperity contacts, and indeed the subdivision of a nanometer contact into numerous atomic-scale contacts may allow the application of the corresponding macro-scale theories.

The results when van der Waals interactions are taken into account are more ambiguous. The authors still find friction to vary in proportion with the real atomic contact area, but this is now a sublinear function of load, leading to friction that can be fitted approximately by the COS equations (an M-D model, Eq. 4). It is suggested that this fit says more about the flexibility of the model, with potentially three fitting parameters, than it does about the physics of contact, an argument made before by Luan and Robbins. In an attempt to demonstrate this, the elastic restoring force $L_{el} = L_{tot} - L_{vdW}$ is calculated as a function of real contact area; assigning the van der Waals contribution a dependence of $A_{real}^{0.51*}$ effectively removes the nonlinearities, and L_{el} is seen to be proportional to the real contact area, allowing interpretation once again in terms of an atomic multi-asperity contact. This is indeed in stark contrast to the Hertz prediction of $A \sim L^{2/3}$, but the authors fail to address the fact that the continuum mechanics model deals with the asperity contact area, not this new atomistic formulation. In the non-adhesive case the asperity contact area was seen to vary roughly in accord with contact mechanics predictions while the real contact area was directly proportional to load; no reasons are presented to suggest this correspondence would be any less valid in the adhesive regime with regard to L_{el}. Still, the net effect of including adhesion is clear, reducing the load dependence of F_{lat} from linear to distinctly sublinear. The authors propose that this transition to sublinearity, observed experimentally and in some MD simulations, is triggered when the range of the attractive interactions approach or exceed the scale of surface roughness and can be achieved in practice by adhesion control (for instance passivation, functionalization or solvent effects).

This last conclusion is entirely reasonable and amply supported by previous experimental and theoretical work. It does not, however, necessitate the much-discussed breakdown of continuum mechanics, reducing as it does to simply another transition parameter between two known continuum regimes (single- versus multi-asperity contact). More significant in that regard is the definition of contact area. Though hardly unprecedented (see, for instance, (37)), this definition is inescapably arbitrary, closely dependent on the choice of cut-off radii and type of interaction considered to the extent that some choice of factors can almost always yield the desired functional dependence. In the words of Mo *et al.*,[49] the friction force is found to be proportional to contact area at all length scales "as long as the contact area is correctly defined at each length scale." And yet, if the definition of contact area cannot remain consistent throughout all relevant length scales, the question remains of whether it actually represents a fundamental quantity. Indeed, the insistence on a contact *area* is particularly troublesome in this case and leads to additional inconsistencies. Many authors have proposed that the number of atoms or molecules interacting across the contact is of prime importance, but assigning each of the contacting atoms an area of interaction is by necessity purely arbitrary. The essence of the issue is that the contact area between two atoms or molecules is, strictly speaking, undefined, suggesting it would be unwise to develop a friction theory based on "real" atomic contact area.

---

* No explanation is provided for the value of this exponent.

The experimental justification for defining contact area in this manner – proportionality to the applied load – also merits closer examination. Multi-asperity and roughness-based contact theories do give a similar load dependence, but the most commonly cited example, the GW model, is explicitly intended for asperities which deform elastically (indeed, which deform according to Hertz contact mechanics). Obviously Mo *et al*. are not proposing the analogous deformation of individual atomic 'asperities', but in the absence of elastic deformation of asperities the GW model is completely inapplicable. Before making the leap from a linear friction-load law to an atomic-level multi-asperity theory, more theoretical work needs to be done to explore the load dependence of these contacts. Finally, it must be pointed out that this is not the only definition of contact area that matches well with simulation data. Luan and Robbins, for instance, found a range of contact radii in (48) much more akin to the "asperity contact radius" that, when squared, all scaled linearly with the simulated friction force. For a different morphology, it was found that a much better description of the friction was afforded by the explicitly incorrect continuum mechanics contact area.[47] Still more variation can be found in the other works cited above, demonstrating the difficulty of consistently defining a contact area at the nanoscale. This leads naturally to the last of the major breakdown studies, in which Gao *et al*. propose that contact area is in many cases neither a fundamental nor necessary quantity.[50]

This observation is grounded in a thorough review of SFA and AFM friction measurements for a broad range of interfaces, which are found to often return comparable friction coefficients for the same materials over length scales differing by multiple orders of magnitude. The primary area dependence clearly identified in the literature is related to the cobblestone model, a purely phenomenological separation of adhesive and load-dependent contributions to friction as $F_{lat} = \mu L + \tau A_{real}$. At low loads, the generally sublinear adhesive term dominates even when very small, but when adhesion is reduced, roughness is increased or higher loads are applied, a linear friction law is almost universally observed. This immediately suggests that the real contact area is completely unimportant for non-adhesive surfaces and may even have little bearing on the frictional behavior of adhesive contacts at high loads. To examine this conclusion, the authors simulated the friction between two gold surfaces, either randomly rough or atomically flat, with an intervening lubricant layer. Because the nature of lubricated contacts is beyond the scope of this paper and the unusually high loads simulated here (an order of magnitude greater than is usual in FFM studies) make comparisons with most systems described above difficult, a detailed discussion of the results is unnecessary. It will be sufficient simply to point out that all simulations returned a linear force-load relation in accordance with Amontons' laws, though this did not hold at small loads, and they agreed generally with experimental data and other simulations.

More relevant here is the analysis of the atomic-level data. As expected from previous discussions, the instantaneous local data for friction and load displayed clear nonlinearities. Such data is generally taken as evidence of the failure of Amontons' laws at the nanoscale, but Gao *et al*.[50] maintain that because the fundamental expression $F_{lat} = \mu L$ is implicitly macroscopic, it entails time- and space-averaged data and cannot be blindly applied to non-macroscopic systems. Indeed, they demonstrate that by averaging the local data over the full simulation time or over the entire surface the linear relation of Amontons' laws can be recovered. This result was replicated with a particularly interesting approach modeling the local normal load and local force data with probability distributions (see Figure 13). In this case the probability density of normal load could be closely fit with a gamma distribution for all but the highest loads, and the local friction versus load data fitted excellently to a Weibull distribution over the entire load range simulated. Because no other tribological systems had been analyzed in this manner, the authors refrained

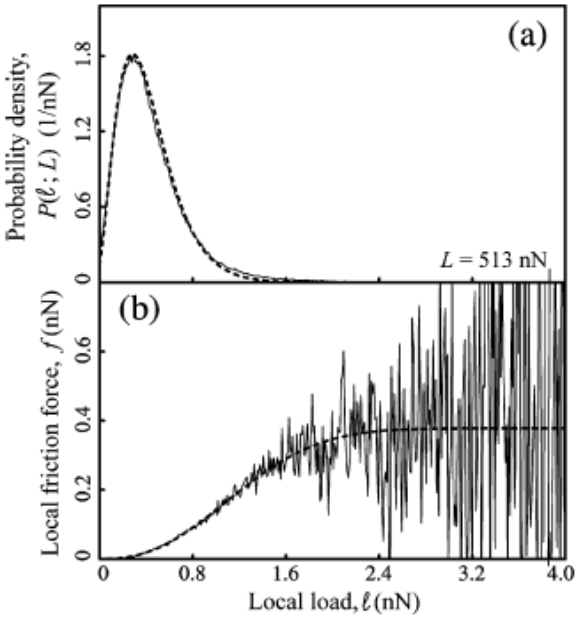

Figure 13. Probability distributions of atomic friction. (a) The probability density of the simulated atomic load, fit closely by a gamma distribution (dotted line). (b) The local friction-load data; though fluctuations are large, the Weibull cumulative distribution function fits the mean excellently. Integrating returns the constant friction coefficient found by MD simulation. From (50)

from drawing any conclusions about the general applicability of these distributions, but the Weibull distribution is especially promising. It was originally developed to model the strengths of materials in which failure of the weakest component leads to complete failure of the material, a system with encouraging parallels to static friction. More recently, it has proven useful for modeling dynamic systems in which multiple bonds are formed and broken, the mechanism most commonly discussed for friction on the nanoscale. Using these two functions to model local friction-load data, Gao *et al.* could precisely recover the macroscopic friction law extracted from the MD simulations. This general technique has potentially powerful implications – by modeling local friction with a probability distribution for the formation and breaking of multiple bonds, it was possible to produce a macroscopic friction law in agreement with experimental data without recourse to the contact area. Indeed, neither approach used by Gao *et al*. made use of the concept of contact area or even defined it. As discussed above, when the mechanism is defined in terms of interactions between individual atoms or molecules, the real contact area is not only undefined but superfluous. It can prove a useful scaling parameter for the truly significant quantity, the number density of bonds formed and broken across the interface, but only in the case of relatively smooth surfaces. More generally, the so-called real contact area can be significantly smaller or greater than the apparent contact area, with a complicated dependence on roughness and adhesion, and the local number density of contacts can fluctuate enormously in both space and time. As such, it is not suitable as a central parameter for theories of friction on the nanoscale.

5 - Conclusions

The final picture of friction on the nanoscale, then, is regrettably unclear, with the only obvious conclusion that much work remains to be done. Certainly the method of Gao *et al.*[50] is compelling, and further investigations should be made using statistical methods to describe friction in terms of atomic or molecular contact without recourse to contact area, with the Weibull as well as other distributions. However, it cannot be ignored that many other simulations and FFM experiments have produced results in general agreement with continuum mechanics models, albeit not always the model initially thought appropriate. This suggests that it would be premature to lay aside continuum-based friction. Many of the factors discussed above such as anisotropy and contact compliance should be able to be incorporated into a new picture of friction. As suggested by Mo *et al.*[49], the balance between single- and multi-asperity-type friction (i.e. sublinear and linear friction-load laws) could be determined by the ratio of surface roughness to the strength of adhesion, a transition parameter analogous to but perhaps more broadly applicable than that of Tabor. This, of course, entails a much more exacting study of surface roughness and its effect on contact and friction. While the statistical effects of multi-asperity contact are generally accepted, the most commonly cited roughness theory, that of GW, is inappropriate at the nanoscale. Further investigations of

Persson's roughness theory and its implications for friction could be fruitful, but this still depends on a concept of contact area, which is once again problematic when roughness is taken to cover atomic length scales. To the extent possible, then, a theory that moved away from Bowden and Tabor friction, with a greater emphasis on roughness distributions and the number of contacts made, would be more promising.

The development of a new model of friction at the nanoscale is only the first step, though – once again, this must be evaluated with cutting-edge AFM and MD techniques. The studies above suggest ample room for improvement in this direction as well. For the evaluation of a nanoscale friction theory, the AFM system must be rigorously characterized to at least that length scale, particularly regarding the roughness and morphology of the tip and surface and the presence of contaminants; this is necessary to avoid applying an inappropriate model due to coincidental functional dependencies. Similarly, as long as the contact area in the AFM remains resistant to characterization, it would be unwise to insert contact area relations into the friction-load data actually produced. For this reason as well, the development of a model of friction that does not depend on contact area would be advantageous. To better understand the precise mechanisms at work, tandem MD simulations will still be necessary, particularly to understand the role of factors such as crystal structure and interface morphology which cannot be included in a continuum model. However, for these results to be more conclusive, simulations must better match experimental data, which will require increased computational power and improved characterization and control of experimental systems. Otherwise, it may continue to remain unclear what breaks down at the nanoscale: continuum mechanics theories of friction, or the misguided application thereof.

6 - References

(1) Delrio, F. W. et al. The role of van der Waals forces in adhesion of micromachined surfaces. Nature Mater. 4, 629–634 (2005).

(2) Bowden, F.P. & Tabor, D. The friction and lubrication of solids. Oxford, Clarendon, UK (1954).

(3) Hertz, H., J. Reine Angew. Math. 92, 156 (1881).

(4) Johnson, K.L., Kendall, K. & Roberts, A.D., Surface energy and the contact of elastic solids. Proc. Roy. Soc. A 324, 301 (1971).

(5) Derjaguin, B.V., Müller, V.M., & Toporov, Y.P., Effect of contact deformations on the adhesion of particles. J. Colloid Interface Sci. 53 (2), 314-326 (1975)

(6) Tabor, D. Surface forces and surface interactions. J. Colloid Interface Sci. 58, 2–13 (1977).

(7) Muller, V. M., Yushenko, V. S., Derjaguin, B. V., On the influence of molecular forces on the deformation of an elastic sphere and its sticking to a rigid plane J. Colloid Interface Sci. 77, 91 (1980).

(8) Hughes, B. D., White, L. R., Soft contact problems in linear elasticity. Q. J. Mech. Appl. Math. 32, 445 (1979).

(9) Maugis, D. Adhesion of spheres—the JKR-DMT transition using a Dugdale model. J. Colloid Interface Sci. 150, 243–269 (1992).

(10) Carpick, R. W., Ogletree, D. F. & Salmeron, M. A general equation for fitting contact area and friction vs load measurements. J. Colloid Interface Sci. 211, 395–400 (1999).

(11) Schwarz, U. D. A generalized analytical model for the elastic deformation of an adhesive contact between a sphere and a flat surface. J. Colloid Interface Sci. 261, 99–106 (2003).

(12) Archard, J.F. Elastic Deformation and the Laws of Friction. Proc. Roy. Soc. A 243, 190 (1957)

(13) Greenwood, J. A. & Williamson, J. B. P. Contact of nominally flat surfaces. Proc. R. Soc. Lond. A 295, 300–319 (1966).

(14) Bush, A. W., Gibson, R. D. & Thomas, T. R. The elastic contact of a rough surface. Wear 35, 87–111 (1975).

(15) Bush, A.W., Gibson, R.D., & Keogh, G.P., Limit of elastic deformation in contact of rough surfaces. Mech. Res. Commun. 3 (3), 169-174 (1976).

(16) Persson, B.N.J., Elastoplastic contact between randomly rough surfaces. Phys. Rev. Lett. 8711 (11), art. no.-116101 (2001).

(17) Persson, B.N.J., Bucher, F., & Chiaia, B., Elastic contact between randomly rough surfaces: Comparison of theory with numerical results. Phys. Rev. B 65, 184106 (2002).

(18) Persson, B.N.J., Relation between interfacial separation and load: a general theory of contact mechanics. Phys Rev Lett 99 (12), 125502 (2007).

(19) Manners, W. & Greenwood, J.A., Some observations on Persson's diffusion theory of elastic contact. Wear 261 (5-6), 600-610 (2006).

(20) Berman, A., Drummond, C. & Israelachvili, J., Amontons' law at the molecular level. Tribology Letters 4, 95 (1998).

(21) Horn, R. G., Israelachvili, J. N. & Pribac, F. Measurement of the deformation and adhesion of solids

in contact. J. Colloid Interface Sci. 115, 480–492 (1987).
(22) Carpick, R. W., & Salmeron, M., Scratching the surface: Fundamental investigations of tribology with atomic force microscopy. Chem. Rev. 97, 1163 (1997).
(23) Schwarz, U.D., Köster, P. & Wiesendanger, R., Quantitative analysis of lateral force microscopy experiments. Rev. Sci. Instrum. 67, 2560 (1996).
(24) Butt, H., Cappella, B. & Kappl, M. Force measurements with the atomic force microscope: Technique, interpretation and applications. Surf. Sci. Reports 59, 1 (2005).
(25) Carpick, R. W., Ogletree, D. F., & Salmeron, M., Lateral stiffness: A new nanomechanical measurement for the determination of shear strengths with friction force microscopy. Appl. Phys. Lett. 70, 1548 (1997).
(26) Lantz, M. A., O'Shea, S. J., Welland, M. E., & Johnson, K. L., Atomic force microscopy study of contact area and friction on $NbSe_2$. Phys. Rev. B 55, 10776 (1997).
(27) Enachescu M., van den Oetelar R. J. A., Carpick R. W., Ogletree D. F., Flipse C. F. J. & Salmeron M., Atomic Force Microscopy Study of an Ideally Hard Contact: The Diamond(111)/Tungsten Carbide Interface. Phys. Rev. Lett. 81, 1877 (2000).
(28) Schwarz, U.D., Zwörner, O., Köster, P. & Wiesendanger R., Quantitative analysis of the frictional properties of solid materials at low loads. I. Carbon compounds. Phys. Rev. B 56, 6987 (1997).
(29) Schwarz, U.D., Zwörner, O., Köster, P. & Wiesendanger R., Quantitative analysis of the frictional properties of solid materials at low loads. II. Mica and germanium sulfide. Phys. Rev. B 56, 6987 (1997).
(30) Schwarz, U.D., Allers, W., Gensterblum, G. & Wiesendanger, R., Low-load friction behavior of epitaxial C_{60} monolayers under Hertzian contact. Phys. Rev. B 52, 14 976 (1995).
(31) Carpick, R.W., Agrait, N., Ogletree, D.F. & Salmeron, M., Measurement of interfacial shear (friction) with an ultra-high vacuum atomic force microscope. J. Vac. Sci. Technol. B 14, 1289 (1996).
(32) Colburn, T. J. & Leggett, G. J. Influence of solvent environment and tip chemistry on the contact mechanics of tip-sample interactions in friction force microscopy of self-assembled monolayers of mercaptoundecanoic acid and dodecanethiol. Langmuir 23, 4959–4964 (2007).
(33) Putman, C. A. J., Igarashi, V. & Kaneko, R. Single-asperity friction in friction force microscopy — The composite-tip model. Appl. Phys. Lett. 66, 3221–3223 (1995).
(34) Hu, J., Xiao, X.-D., Ogletree, D.F. & Salmeron, M., Atomic-scale friction and wear of mica. Surf. Sci. 327, 358 (1995).
(35) Gao, G. T., Cannara, R. J., Carpick, R. W. & Harrison, J. A. Atomic-scale friction on diamond: a comparison of different sliding directions on (001) and (111) surfaces using MD and AFM. Langmuir 23, 5394–5405 (2007).
(36) Riedo, E., Chevrier, J., Comin, F. & Brune, H. Nanotribology of carbon based thin films: The influence of film structure and surface morphology. Surf. Sci. 477, 25–34 (2001).
(37) Brukman, M.J., Gao, G., Nemanich, R.J. & Harrison, J.A. Temperature dependence of single-asperity diamond-diamond friction elucidated using AFM and MD simulations. J. Phys. Chem. C 112, 9358 (2008).
(38) Brenner, D.W., Empirical potential for hydrocarbons for use in simulating the chemical vapor deposition of diamond films. Physical Review B 42 (15), 9458 (1990).
(39) Brenner, D. et al. A second-generation reactive empirical bond order (REBO) potential energy expression for hydrocarbons. J. Phys. Condens. Matter 14, 783–802 (2002).
(40) Stuart, S.J., Tutein, A.B., & Harrison, J.A., A reactive potential for hydrocarbons with intermolecular interactions. J. Chem. Phys. 112 (14), 6472-6486 (2000).
(41) Dienwiebel, M., Verhoeven, G.S., Pradeep, N., Frenken, J.W.M., Heimberg, J.A. & Zandbergen, H.W. Superlubricity of graphite. Phys. Rev. Lett. 92, 126101 (2004).
(42) Robbins, M.O. & Smith, E.D. Connecting molecular-scale and macroscopic tribology. Langmuir 12, 4543 (1996).
(43) He, G., Müser, M.H. & Robbins, M.O. Adsorbed Layers and the Origin of Static Friction. Science 284, 1650 (1999).
(44) He, G. & Robbins, M.O. Simulations of the static friction due to adsorbed molecules. Phys. Rev. B 64, 035413 (2001).
(45) Müser, M.H., Wenning, L. & Robbins, M.O., Simple microscopic theory of Amontons's laws for static friction. Phys. Rev. Lett. 86, 1295 (2001).
(46) Wenning, L. & Müser, M. H. Friction laws for elastic nanoscale contacts. Europhys. Lett. 54, 693–699 (2001).
(47) Luan, B. & Robbins, M. O. The breakdown of continuum models for mechanical contacts. Nature 435, 929–932 (2005).
(48) Luan, B. & Robbins, M. O. Contact of single asperities with varying adhesion: comparing continuum mechanics to atomistic simulations. Phys. Rev. E 74, 026111 (2006).
(49) Mo, Y., Turner, K. & Szlufarska, I. Friction laws at the nanoscale. Nature 457, 1116-1119 (2009).
(50) Gao, J., Luedtke, W.D., Gourdon, D., Ruths, M., Israelachvili, J. Landman, U., Frictional forces and Amontons' law: from the molecular to the macroscopic scale. J. Phys. Chem. 108, 3410–3425 (2004).